

# 热管换热器内部流动与换热的数值模拟

徐洪宝, 孙 铁, 杨雪峰

(辽宁石油化工大学 机械工程学院 辽宁 抚顺 113001)

**摘 要:** 单螺旋翅片热管管束的翅片结构中心对称处存在流体流动及换热不足, 因此, 将单螺旋翅片结构改为新型双螺旋翅片结构, 并利用 Fluent 软件模拟分析改进后流场与温度场的变化情况。结果表明: 在  $Re = 500 \sim 6\,500$  时, 与未加翅片相比, 单螺旋翅片热管换热增强 33% ~ 51%, 摩擦阻力系数增加 6% ~ 24%; 双螺旋翅片热管换热增强 69% ~ 84%, 摩擦阻力系数增加 19% ~ 48%。且双螺旋结构的综合性能明显优于单螺旋结构的综合性能, 且在  $Re = 2\,000$  时性能表现最优。根据场协同原理可知, 双螺旋翅片结构对流体强烈扰动可促使流体的速度矢量与温度梯度矢量协同程度更好。综合比较得知双螺旋翅片热管更有利于强化换热。

**关 键 词:** 双螺旋翅片; 热管; 场协同原理; 数值模拟

中图分类号: TK124 文献标识码: A

DOI: 10.16146/j.cnki.rndlgc.2016.09.004

## 引 言

自二十世纪六十年代热管问世以来, 工程师们已经将热管技术广泛地应用到人民生活息息相关的各行各业中, 尤其在低温余热回收领域, 热管技术广受青睐<sup>[1]</sup>。由热管组成的换热器不仅可以回收余热以供人类再次利用, 并且有效地降低烟气余热所造成的热污染。但是在余热回收时, 由于烟气或气体通过换热器管束时表面换热系数较低, 因此各种强化传热技术应用到热管换热器中<sup>[2]</sup>。翅片(又称肋片)是一种常见的强化传热技术, 特别是在对流传热系数较弱的一侧采用翅化表面可以有效的强化换热, 因而许多工程师及科研人员对加装翅片热管换热器进行了理论、实验和数值模拟研究<sup>[3~11]</sup>。但对螺旋翅片的数值模拟研究相对较少或模型简化较大(主要简化成环形翅片), 所以利用 Fluent 软件通过计算机数值模拟的方法, 对螺旋翅片热管换热器

冷却段进行三维数值模拟, 直观的观察螺旋翅片热管换热器内部的流动与换热情况, 分析不同模型的温度场和速度场的协同关系, 在此基础上提出一种新型翅片模型—双螺旋翅片。

## 1 数值计算模型

### 1.1 几何模型

利用 Fluent 软件分别模拟了未加装翅片、单螺旋翅片和双螺旋翅片热管换热器流场和温度场变化情况, 管束排列方式为错排排列。图 1 为双螺旋翅片热管结构, 图 2 为换热器模型结构简图, 翅片参数如表 1 所示。本例三种模型的网格划分已经过网格无关性检验, 综合考虑计算机性能与计算时间的限制, 划分的三种模型网格数量大约为 200 万个。

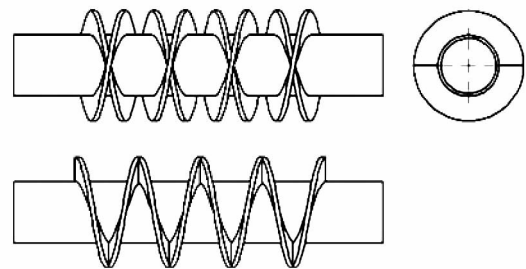


图 1 双螺旋翅片热管结构

Fig. 1 Dual spiral fin structure

表 1 双螺旋翅片结构参数

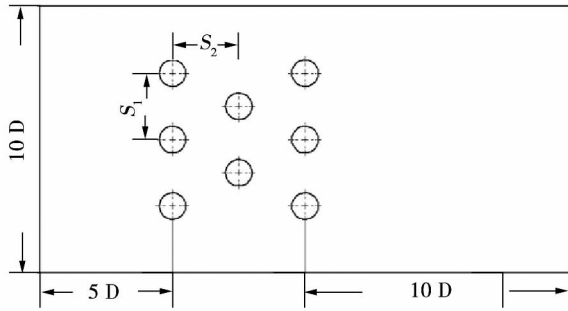
Tab. 1 Structural parameters of a dual spiral fin

热管外径	热管长度	翅片高度	翅片厚度	翅片螺距	翅片数目
20 mm	120 mm	8 mm	1.5 mm	20 mm	4 个

收稿日期: 2015-10-30; 修订日期: 2015-12-14

基金项目: 辽宁省自然科学基金项目 (2013020117)

作者简介: 徐洪宝(1990-), 男, 辽宁营口人, 辽宁石油化工大学硕士研究生。



注:  $D$ —热管直径;  $S_1$ —横向间距;  $S_2$ —纵向间距

图 2 热管换热器结构简图

Fig. 2 Simplified drawing of the structure of a heat pipe heat exchanger

### 1.2 数学模型

在三维直角坐标系中,对流传热的控制方程有连续方程、动量方程、能量方程和状态方程组成,其矢量形式表示如下:

连续性方程:

$$\frac{\partial \rho}{\partial t} + \frac{\partial(\rho u)}{\partial x} + \frac{\partial(\rho v)}{\partial y} + \frac{\partial(\rho w)}{\partial z} = 0 \quad (1)$$

$x$  动量方程:

$$\frac{\partial(\rho u)}{\partial t} + \text{div}(\rho u \vec{u}) = \text{div}(\mu \text{grad} u) - \frac{\partial p}{\partial x} + S_u \quad (2)$$

$y$  动量方程:

$$\frac{\partial(\rho v)}{\partial t} + \text{div}(\rho v \vec{u}) = \text{div}(\mu \text{grad} v) - \frac{\partial p}{\partial y} + S_v \quad (3)$$

$z$  动量方程:

$$\frac{\partial(\rho w)}{\partial t} + \text{div}(\rho w \vec{u}) = \text{div}(\mu \text{grad} w) - \frac{\partial p}{\partial z} + S_w \quad (4)$$

能量方程:

$$\frac{\partial(\rho T)}{\partial t} + \text{div}(\rho u T) = \text{div}\left(\frac{K}{C_p} \text{grad} T\right) + S_T \quad (5)$$

气体状态方程:

$$\rho = f(P, T) \quad (6)$$

式中,  $\rho$ —密度,  $\text{kg}/\text{m}^3$ ;  $t$ —时间,  $\text{s}$ ;  $u, v$  和  $w$ —速度矢量  $\vec{u}$  在  $x, y$  和  $z$  方向的分量,  $\text{m}/\text{s}$ ;  $P$ —压力,  $\text{Pa}$ ;  $\mu$ —动力粘度,  $\text{Pa} \cdot \text{s}$ ;  $S_u, S_v$  和  $S_w$ —动量守恒方程的广义源项;  $C_p$ —定压比热容,  $\text{J}/(\text{kg} \cdot \text{K})$ ;  $T$ —温度,  $\text{K}$ ;  $K$ —流体的传热系数,  $\text{W}/(\text{m}^2 \cdot \text{K})$ ;  $S_T$ —粘性耗散。

## 2 边界条件和数值模拟算法的设置

### 2.1 边界条件设置:

(1) 计算模型的入口设置为速度入口边界条件,入口温度为  $303.15 \text{ K}$ ; (2) 出口设置为压力出口边界条件; (3) 热管具有超导特性,因此将热管模型简化为定壁温,翅片材料一般为铜或铝,导热系数较大,因此将壁面与翅片同时设定为恒温边界条件,温度为  $473.15 \text{ K}$ ; (4) 外壁面采用相同的速度随流体流动,这样可以避免壁面处边界层对计算产生的影响,温度设置为绝热边界条件; (5) 由于流体温度范围变化较大,因此采用变物性参数,通过 UDF 编程将编写的程序导入 Fluent 软件中进行解释或编译,同时考虑重力对流动产生的影响,重力加速度为  $9.8 \text{ m}/\text{s}^2$  沿  $Z$  轴负向。

### 2.2 数值模拟算法设置:

利用有限体积法离散控制方程,选用标准  $k - \varepsilon$  湍流模型,动量、能量和湍流参量等方程的离散均采用二阶迎风格式,由于三种模型的无量纲距离  $Y^+ = 1 \sim 5$ ,因此对近壁面处理采用增强壁面函数,压力与速度的耦合计算采用 SIMPLEC 算法,选取稳态格式进行求解。

## 3 数据处理

表面换热系数  $h$ :

$$h = \frac{q}{T_w - T_{\text{ref}}}$$

式中:  $q$ —流体热流密度,  $\text{W}/\text{m}^2$ ;  $T_w$ —热管壁面温度,  $\text{K}$ ;  $T_{\text{ref}}$ —流体参考温度,选取膜温为参考温度,  $\text{K}$ 。

传热  $Nu_0$  数:

$$Nu_0 = \frac{h_0 d_0}{\lambda}$$

式中:  $h_0$ —以热管基管外表面为基准的表面换热系数,  $\text{W}/(\text{m}^2 \cdot \text{K})$ ;  $\lambda$ —空气导热系数,  $\text{W}/(\text{m} \cdot \text{K})$ ;  $d_0$ —热管外径,  $\text{m}$ 。

$$h_0 = h \eta \beta$$

式中:  $\eta$ —翅片热管的翅片效率<sup>[12]</sup>,  $\beta$ —翅片热管的翅化比。

雷诺数  $Re$ :

$$Re = \frac{u_{max} d_0}{\nu}$$

式中:  $u_{max}$ —换热器最小流通截面处的平均速度, m/s;  $\nu$ —空气的运动粘度,  $m^2/s$ 。

摩擦阻力系数  $f$ :

$$f = \frac{2 d_0 \Delta p}{L u_{max}^2 \rho}$$

式中:  $\Delta p$ —沿程压降, Pa;  $L$ —流程长度, m;  $\rho$ —流体密度,  $kg/m^3$ 。

### 4 结果分析

数值计算后得到的未加翅片、单螺旋翅片和双螺旋翅片热管管束的平均摩擦阻力系数和平均努塞尔数图如图 3、图 4 所示。在  $Re = 500 \sim 6500$  时 结果发现与未加翅片即光滑圆管相比, 单螺旋翅片热管换热可增强 33% ~ 51%, 摩擦阻力系数增加 6% ~ 24%; 双螺旋翅片热管换热可增强 69% ~ 84%, 摩擦阻力系数增加 19% ~ 48%。

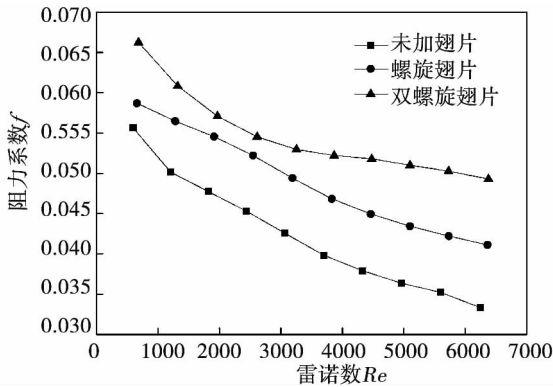


图 3 数值计算后未加翅片、单螺旋翅片和双螺旋翅片热管管束的平均摩擦阻力系数

Fig. 3 Average friction resistance coefficient of a no - fin installed single spirally finned and dual spirally finned heat pipe bundle after the numerical calculation

#### 4.1 换热分析

以进口速度 2.0 m/s 为例, 分别选取垂直于  $Z$  轴的三个截面  $Z = 0.024\text{ m}$ ,  $Z = 0.028\text{ m}$  和  $Z = 0.036\text{ m}$  观察其温度场变化情况, 以及垂直于  $X$  轴的截面  $X = 0\text{ m}$  观察其流场变化情况进一步说明换热增强的原因。其中未加翅片的温度场变化如图 5

所示, 因其它截面变化大致相同, 只选取截面  $Z = 0.024\text{ m}$ 。流体扰流热管时在热管背风侧由于压差形成漩涡, 而对于纵向截面如图 6 所示, 速度分量垂直于热管壁面并未形成纵向漩涡未能对流体以及边界层进行充分的扰动, 所以等温线并不均匀主要集中在热管壁面处。

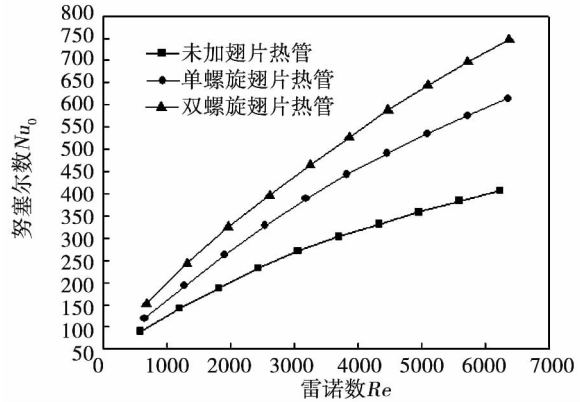


图 4 数值计算后未加翅片、单螺旋翅片和双螺旋翅片热管管束的平均努塞尔数

Fig. 4 Average Nu number of a no - fin installed, single spirally finned and dual spirally finned heat pipe bundle after the numerical calculation

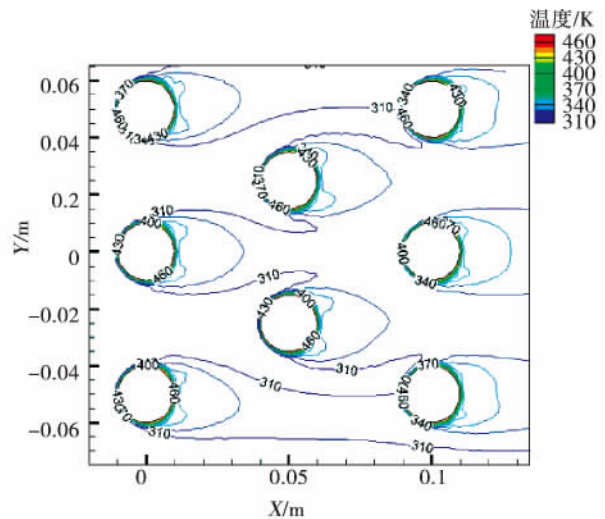


图 5 未加翅片  $Z = 0.024\text{ m}$  截面局部温度场

Fig. 5 Local temperature field in a cross section of  $Z = 0.024\text{ m}$  when no fins are additionally installed

单螺旋翅片结构流体的温度场较未加翅片时流体的温度场已有了较大的改变如图 9、图 11 与图 13 所示。这是因为单螺旋翅片增加了二次传热表面,

加强了对流体扰流热管的干扰,破化了原来未强化的流体的速度分布和温度分布场。流体扰流热管时热管壁面使流体产生分流,同时由于单螺旋具有一定的倾斜角度使流体产生偏离主流方向的流动,并且在翅片下表面处压强较低而周围流体压强较高,这使流体产生回流形成漩涡,所以斜向偏离的流体速度与沿管壁的流体速度相互叠加和压差产生纵向漩涡,如图 7 所示。光管处边界层的形成与发展不断被破坏同时也对周围流体产生强烈扰动,这样使得温度场比未加翅片时流体的温度场有了较大的改变。

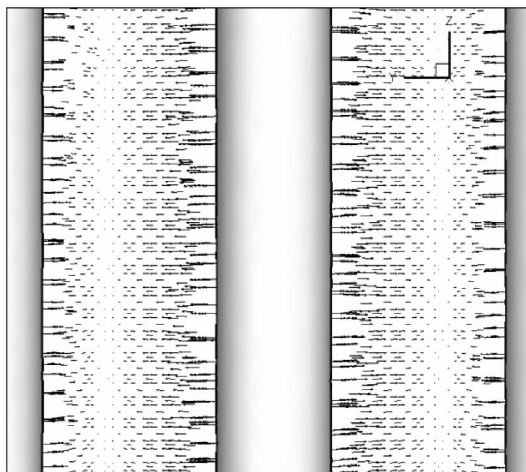


图 6 未加翅片  $X = 0\text{ m}$  截面局部流场  
Fig. 6 Local flow field in a cross section of  $X = 0\text{ m}$  when no fins are additionally installed

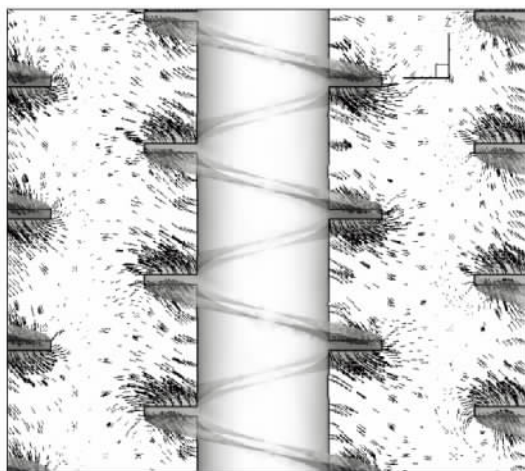


图 7 单螺旋翅片  $X = 0\text{ m}$  截面局部流场  
Fig. 7 Local flow field in a cross section of  $X = 0\text{ m}$  when single spiral fins are used

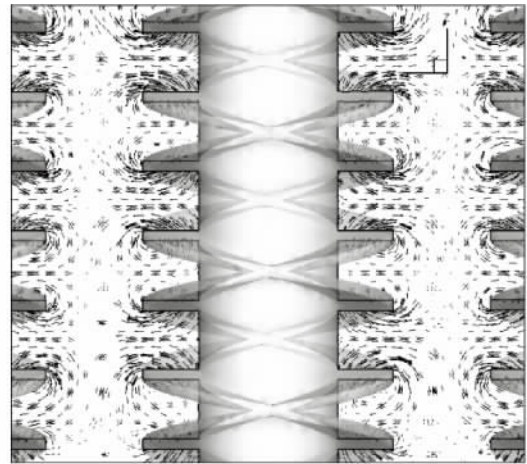


图 8 双螺旋翅片  $X = 0\text{ m}$  截面局部流场  
Fig. 8 Local flow field in a cross section of  $X = 0\text{ m}$  when dual spiral fins are used

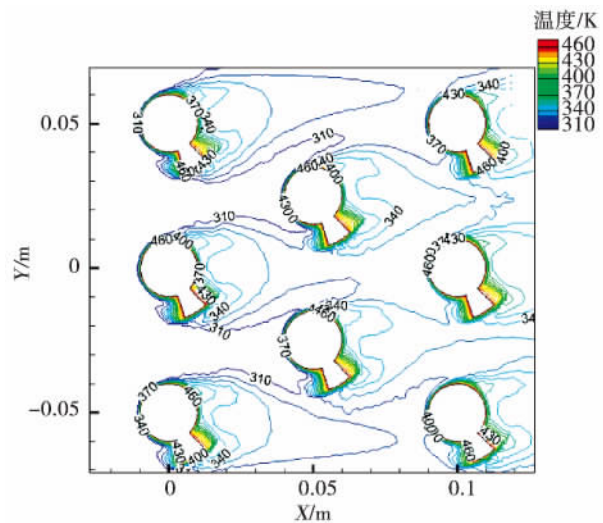


图 9 单螺旋翅片  $Z = 0.024\text{ m}$  截面局部温度场  
Fig. 9 Local temperature field in a cross section of  $Z = 0.024\text{ m}$  when single spiral fins are used

但是,单螺旋结构在每根热管中心在  $XOZ$  面对称处流体流动与壁面边界层并未得到充分干扰和破坏,该处流体等温线变化与未加翅片结构的等温线变化大致相同,需要极大的改善此处流体的扰动来增强换热,因此通过对单螺旋翅片结构的改变形成双螺旋翅片结构。双螺旋结构为两个螺旋方向相反的单螺旋组成,具有关于中心对称结构恰好弥补了单螺旋结构对流体扰动的不足。双螺旋结构比单螺旋结构不仅更大的增加了二次传热表面同时对周围流体的扰动明显强于未加翅片结构和单螺旋结构对流体的影响如图 8 所示。双螺旋结构使流体产生的

纵向漩涡明显优于单螺旋对流体的扰动,强烈的纵向漩涡使流体的温度场发生显著的变化如图 10、图 12 和图 14 所示。在具有单螺旋结构优点的同时,沿着热管方向双螺旋还具有渐扩与渐缩结构,对热管壁面与翅片上下表面和周围管束有强烈的冲刷作用,不断地破坏边界层的形成与发展,使不同截面处的等温线较未加翅片和单螺旋翅片的等温线更均匀。

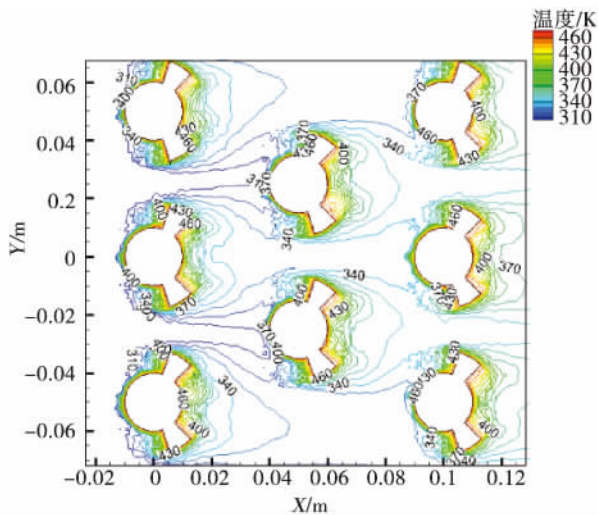


图 10 双螺旋翅片  $Z = 0.024 \text{ m}$  截面局部温度场  
Fig. 10 Local temperature field in a cross section of  $Z = 0.024 \text{ m}$  when dual spiral fins are used

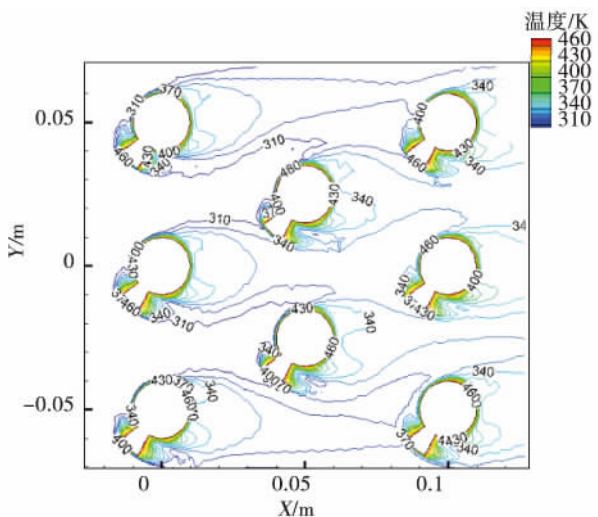


图 11 单螺旋翅片  $Z = 0.028 \text{ m}$  截面局部温度场  
Fig. 11 Local temperature field in a cross section of  $Z = 0.028 \text{ m}$  when single spiral fins are used

#### 4.2 阻力分析

双螺旋翅片热管使流体换热能力增强,同时也

会产生较大的阻力,这是因为与未加翅片和单螺旋翅片结构相比双螺旋翅片结构在迎风面处具有较大的驻点面积。由于驻点是速度为零的点,这使得更多的速度能量转变为压强能量,进而产生较大的压差阻力。其次当粘性流体流过换热面表面时产生很薄的边界层,在边界层内粘性力起主导作用因而产生粘性阻力,而双螺旋结构具有更大的二次换热面积因此具有较大的粘性阻力。同时双螺旋结构是由热管和旋转方向不同的两个单螺旋组成,每个部件放在流体中都会产生阻力,而每个部件产生的阻力又会相互作用,所以在它周围所产生的阻力要比每个部件单独放在流体中产生的阻力总和更大也更复杂,另外当流体扰流物体时会在背风侧形成压力差产生漩涡,漩涡能量逐渐耗散在粘性流体中,产生比未加翅片和单螺旋翅片结构较大的诱导阻力。因此,双螺旋结构产生的阻力大于其他两种模型产出的阻力。

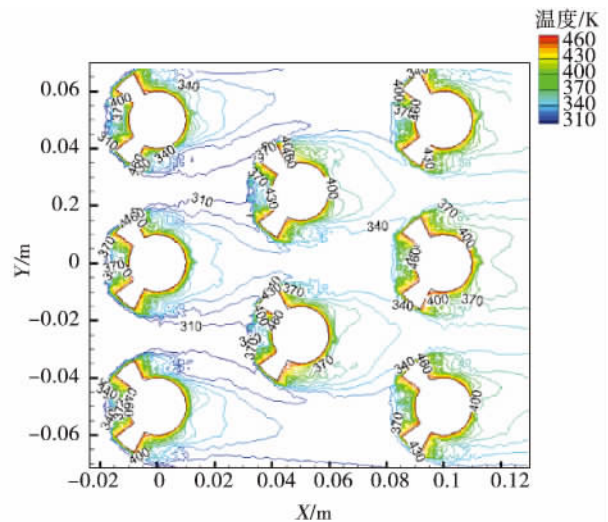


图 12 双螺旋翅片  $Z = 0.028 \text{ m}$  截面局部温度场  
Fig. 12 Local temperature field in a cross section of  $Z = 0.028 \text{ m}$  when dual spiral fins are used

#### 4.3 综合性能分析

双螺旋结构虽然增强传热,但阻力也相应增加。为了综合比较换热性能,采用威伯提出的一套较为完整的综合性能评价准则— $PEC = \left( \frac{Nu_e}{Nu_s} \right) / \left( \frac{f_e}{f_s} \right)^{1/3}$  [13],

其值大于 1 时表明在相同输送功率下,强化传递的热量比光管多。对三种模型的热管换热器进行综合性能分析如图 15 所示,结果表明在相同输送功率下,单螺旋翅片热管与双螺旋翅片热管传递的热量均比未加翅片热管传递的热量多,并且双螺旋翅片

热管综合性能明显优于单螺旋翅片热管。单螺旋翅片热管的综合性能在  $Re = 500 \sim 4\,000$  时几乎成线性增长,并随着雷诺数的增大,性能逐渐趋于平缓;双螺旋翅片热管的综合性能随着雷诺数的增加整体上大致相同,但在  $Re = 1\,300 \sim 2\,400$  时综合性能出现波动,在  $Re = 2\,000$  时性能表现最优,之后随着雷诺数的增加,综合性能有所降低但不久后性能缓慢而平稳的增加,综合比较发现双螺旋翅片热管更有利于强化传热。

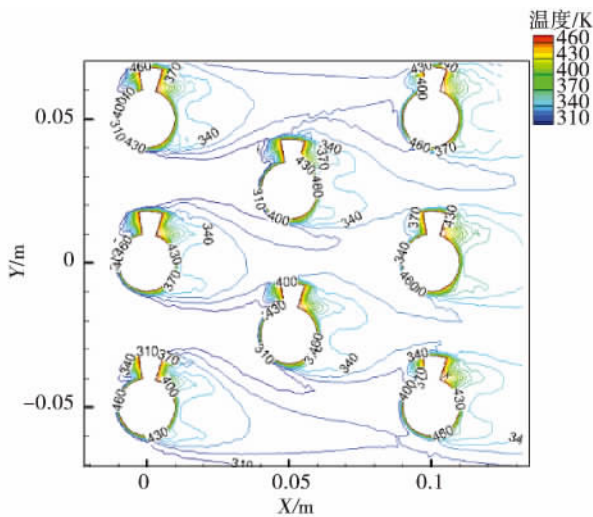


图 13 单螺旋翅片  $Z = 0.036\text{ m}$  截面局部温度场  
Fig. 13 Local temperature field in a cross section of  $Z = 0.036\text{ m}$  when single spiral fins are used

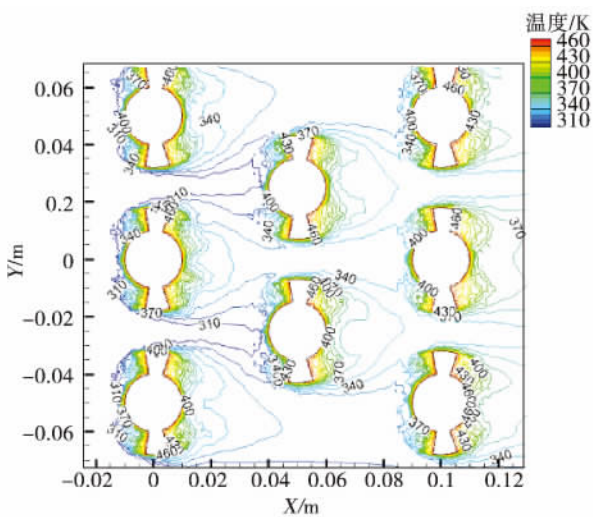


图 14 双螺旋翅片  $Z = 0.036\text{ m}$  截面局部温度场  
Fig. 14 Local temperature field in a cross section of  $Z = 0.036\text{ m}$  when dual spiral fins are used

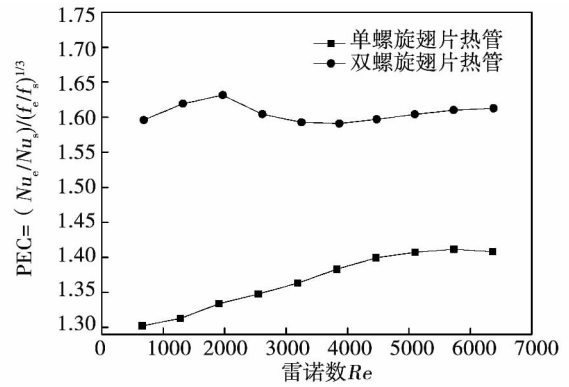


图 15 不同翅片换热与阻力性能的比较  
Fig. 15 Comparison of the heat exchange and resistance performance of various fins

#### 4.4 传热强化原理

从场协同数  $F_c = \int \bar{U} \cdot \nabla T d\bar{y} = \frac{Nu}{RePr}$  定义知<sup>[14]</sup> 场协同数代表了流场与温度场的协同程度,其值永远小于 1,  $F_c = 1$  为理想情况下的完全协同数。当场协同数越接近理想情况下的完全协同时,流场与温度场的协同程度越好。而对流传热特性不仅取决于流体速度、流体与壁面温差、流体的热物理性质,而且还取决于速度矢量与温度梯度矢量之间的角度即协同程度。图 16 对三种模型相互比较得知,单螺旋翅片结构热管管束与双螺旋翅片结构热管管束对流体的扰动均强于未加翅片的光滑热管管束对流体的扰动,而双螺旋翅片热管对流体扰动最强,速度矢量与温度梯度矢量的协同程度均优于其他两种模型的协同程度。正是双螺旋结构使协同程度发生了微小变化,使流体换热性能明显改变,从而达到了强化换热的目的。

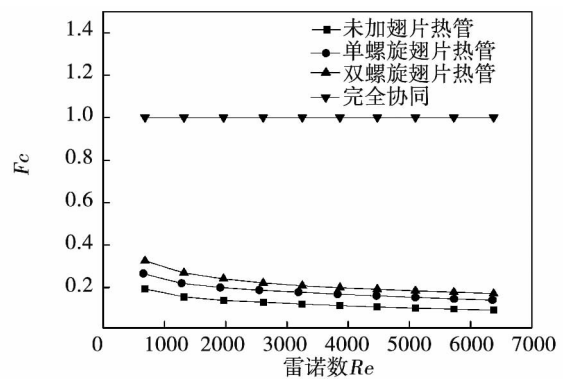


图 16 不同对流传热情况的场协同数  
Fig. 16 Field synergy numbers under various convective heat transfer conditions

## 5 结 论

通过对改进的双螺旋翅片结构进行模拟得知,在  $Re = 500 \sim 6\ 500$  时,与未加翅片相比,单螺旋翅片热管换热可增强 33% ~ 51%,摩擦阻力系数增加 6% ~ 24%;双螺旋翅片热管换热可增强 69% ~ 84%,摩擦阻力系数增加 19% ~ 48%。单螺旋翅片结构和双螺旋结构的换热效果均强于未加翅片结构的换热效果,双螺旋翅片结构的综合性能明显优于单螺旋结构的综合性能,并在  $Re = 2\ 000$  时综合性能表现最优。通过场协同数得知,双螺旋结构使流体的速度矢量与温度梯度矢量的协同程度均优于其它两种模型的协同程度,这是因为双螺旋结构为两个螺旋方向相反的单螺旋组成,具有关于中心对称结构,可以对流经热管两旁的流体同时干扰,增强周围流体的二次流动,使协同程度的少许改善,可使换热显著增强,达到了强化传热的目的。综合比较得知改进的双螺旋翅片结构更有利于强化传热。另外也应综合选择换热增强所带来的能量损耗。

### 参考文献:

- [1] 王斌斌,仇性启. 热管及其换热器在烟气余热回收中的应用[J]. 工业加热 2006 35(5): 36-40.  
WANG Bin-bin, QIU Xing-qi. Applications of heat pipes and their heat exchangers in waste heat recovery from flue gases[J]. Industrial Heating 2006 35(5): 36-40.
- [2] 李安军,邢桂菊,周丽雯. 换热器强化传热技术的研究进展[J]. 冶金能源 2008 27(1): 50-54.  
LI An-jun, XING Gui-ju, ZHOU Li-wen. Progress in the study of the intensified heat transfer technologies for heat exchangers[J]. Metallurgical Energy Source 2008 27(1): 50-54.
- [3] 赵蔚琳. 高温热管翅性能及其强化传热过程的研究[D]. 江苏: 南京工业大学 2004.  
ZHAO Wei-lin. Study of the performance and intensified heat transfer process of fins on high temperature heat pipes[D]. Jiangsu: Nanjing University of Technology 2004.
- [4] 马有福,袁益超,陈昱等. 翅片螺距对锯齿螺旋翅片热管特性的影响[J]. 化工学报 2011 62(9): 2484-2489.  
MA You-fu, YUAN Yi-chao, CHEN Yu, et al. Effects of the fin pitch on the characteristics of a serrated spirally-finned heat exchange tube[J]. Journal of Chemical Industry 2011 62(9): 2484-2489.
- [5] 王鑫煜. 内螺纹重力热管强化传热特性研究[D]. 山东: 山东大学 2013.  
WANG Xin-yu. Study of the intensified heat transfer characteristics of an internally threaded gravity heat pipe[D]. Shandong: Shandong University 2013.
- [6] 袁益超,刘聿拯,曹建光. 螺旋鳍片管束传热与阻力特性研究的现状与发展[J]. 动力工程 2002 22(5): 1922-1927.  
YUAN Yi-chao, LIU Yu-zheng, CAO Jian-guang. Status quo and development of the study of the heat transfer and resistance characteristics of spirally finned tubes[J]. Power Engineering 2002 22(5): 1922-1927.
- [7] 曹双俊. 新型重力热管换热器性能实验及数值研究[D]. 湖南: 中南大学 2011.  
CAO Shuang-jun. Experimental and numerical investigation of the performance of a novel gravity heat pipe heat exchanger[D]. Hunan: Central South University 2011.
- [8] 何雅玲,楚攀,谢涛. 纵向涡发生器在管式换热器中的应用及优化[J]. 化工学报 2012 63(3): 746-760.  
HE Ya-ling, CHU Pan, XIE Tao. Applications and optimization of longitudinal vortex generators in tube type heat exchangers[J]. Journal of Chemical Industry 2012 63(3): 746-760.
- [9] 张亚君,黄德斌,潘朝群等. 气流横向冲刷圆壳管束的传热实验研究[J]. 化学工程 2006 34(11): 12-15.  
ZHANG Ya-jun, HUANG De-bin, PAN Zhao-qun, et al. Experimental study of the heat transfer of a gas flow laterally sweeping across a circular shell tube bundle[J]. Chemical Engineering, 2006 34(11): 12-15.
- [10] 苟秋平,吴学红,吕彦力等. 复合翅片传热与流动特性的数值模拟[J]. 热科学与技术 2011 10(4): 317-323.  
GOU Qiu-ping, WU Xue-hong, LYU Yan-li, et al. Numerical simulation of the heat transfer and flow characteristics of a complex fin[J]. Thermal Science and Technology 2011 10(4): 317-323.
- [11] Qu Z G, Tao W Q, He Y L. Three-dimensional numerical simulation on laminar heat transfer and fluid flow characteristics of strip fin surface with X-arrangement of strips[J]. Heat Transfer 2004, 126(5): 697-707.
- [12] 刘纪福,于洪伟. 环形翅片效率的简化计算方法[J]. 节能技术 2011 29(167): 245-247.  
LIU Ji-fu, YU Hong-wei. A simplified method for calculating the efficiency of an annular fin[J]. Energy Conservation Technology, 2011 29(167): 245-247.
- [13] Webb R L. Performance evaluation criteria for use of enhance heat transfer surfaces in heat exchanger design[J]. Heat and Mass Transfer. 1981 24(4): 715-726.
- [14] 李志信,过增元. 对流传热优化的场协同理论[M]. 北京: 科学出版社 2010.  
LI Zhi-xin, GUO Zeng-yuan. Field synergy theory for optimizing the convective heat transfer[M]. Beijing: Science Press 2010.

(刘瑶 编辑)

change however, the pressure drop will also increase accordingly. **Key words:** foam metal, nano-fluid, intensified heat exchange, numerical simulation

横纹槽管内插断续扭带复合强化传热的实验研究 = **Experimental Study of the Complex Intensified Heat Transfer by Intermittently Inserting Twisted Strips into a Transversely Slotted Tube** [刊, 汉]/LEI Shi-yi, GUO Ya-jun ( College of Environmental and Municipal Engineering, Xi'an University of Architectural Science and Technology, Xi'an, China, Post Code: 710055), GUI Miao, BI Qin-cheng ( National Key Laboratory on Multi-phase Flow in Power Engineering, Xi'an Jiaotong University, Xi'an, China, Post Code: 710049) //Journal of Engineering for Thermal Energy & Power. -2016, 31(9). -15 ~ 19

An experiment was performed with a heat-conduction oil serving as the working medium. In a range of the Re number between the laminar flows and transition flows ( $Re < 7000$ ), the flow and intensified heat exchange characteristics of a transversely slotted tube internally inserted with intermittent twisted strips in three different specifications and continuous twisted strips at the same twist rate ( $Y = 4.13$ ) were investigated. Experimental correlation formulae of the resistance coefficient and the Nu number were obtained respectively by performing a regressive analysis of the test data, thus offering a theoretical basis for calculating the complex intensified heat transfer. It has been found that the comprehensive heat exchange performance of a transversely slotted tube internally inserted with the twisted strips is superior to that of a bare tube internally inserted with the same twisted strips. The comprehensive heat exchange performance of a transversely slotted tube internally inserted with the intermittent twisted strips in a length of 66 mm is superior to that internally inserted with the continuous twisted strips. The test results can provide a theoretical basis for the reconstruction of heat exchangers and design of novel heat exchangers. **Key words:** transversely slotted tube, intermittently twisted strip, complex intensified heat transfer, performance evaluation coefficient (PEC), resistance characteristics

热管换热器内部流动与换热的数值模拟 = **Numerical Simulation of the Flow and Heat Exchange Inside a Heat Pipe Heat Exchanger** [刊, 汉]/XU Hong-bao, SUN Tie, YANG Xue-feng ( College of Mechanical Engineering, Liaoning Petroleum and Chemical Engineering University, Fushun, China, Post Code: 113001) //Journal of Engineering for Thermal Energy & Power. -2016, 31(9). -20 ~ 26

There exists a poor flow and insufficient heat exchange of the fluid at the structural center of the fin in a single helically finned heat pipe tube bundle. As a result, the single helical fin structure was replaced by the novel dual helical fin structure and the flow field and temperature field after the improvement were simulated and analyzed by using the software Fluent. It has been found that when  $Re = 500 \sim 6500$ , compared with a heat pipe not installed with fins, the heat quantity exchanged by a heat pipe additionally installed with single helical fins will enhance by 33% to 51% and the friction resistance coefficient will increase by 6% to 24% while the heat quantity exchanged by a heat pipe additionally installed with the dual helical fins will enhance by 69% to 84% and the friction resistance

coefficient will increase by 19% to 48%. In addition, the comprehensive performance of the dual helical structure will be obviously superior to that of the single helical structure and the comprehensive performance of the dual helical structure will attain its optimum when  $Re = 2\ 000$ . It can be known from the field synergy principles that the intense disturbance to the fluid caused by the dual helical fin structure will force the synergy degree of the speed vector and the temperature gradient vector of the fluid to become better. The comprehensive comparison results show that the dual helically finned heat pipe is more instrumental to enhancing the heat exchange. **Key words:** dual helical fin heat pipe, numerical simulation, field synergy principle

乙醇胺水溶液降膜吸收  $\text{CO}_2$  的数值研究 = **Numerical Study of the Falling Film Absorption of Carbon Dioxide by Monoethanolamine Solution** [刊, 汉] / ZHAO Lin-lin, DING Yu-dong, ZHU Xun, LIAO Qiang ( Education Ministry Key Laboratory on Low-grade Energy Source Utilization Technologies and Systems, Chongqing University, Chongqing, China, Post Code: 400030) // Journal of Engineering for Thermal Energy & Power. - 2016, 31(9). - 27 ~ 32

In the light of the heat and mass transfer problems in the process of the MEA ( monoethanolamine) solution to absorb the carbon dioxide in falling films, a two-dimensional mathematical model for the MEA solution at various concentrations absorbing carbon dioxide in falling films was established and the distribution of both temperature and concentration field inside the liquid films as well as the law governing changes of the heat flux, mass flux and carbon dioxide absorption rate inside the liquid films along the liquid film falling direction were obtained. It has been found that the temperature at the inlet on the boundary surface rapidly increases and then assumes a decline as per an exponential regularity. The heat flux, mass flux and carbon dioxide absorption rate along the liquid film falling direction at the inlet drops sharply like a straight line and afterwards, changes by a small margin, indicating that the absorption action mainly happens at places closing to the inlet section. At the middle location of the liquid film, the variation tendency of the heat and mass flux differs greatly around the inlet section, which is possibly caused by a part of the reaction-released heat quantity absorbed by the liquid. **Key words:** monoethanolamine solution, falling film absorption, two-dimensional numerical simulation, heat flux, mass flux

微通道内表面活性剂水溶液饱和流动沸腾换热特性的数值模拟 = **Numerical Simulation of the Saturated Flow Boiling Heat Exchange Characteristics of a Surfactant Water Solution in a Microchannel** [刊, 汉] / WANG Ying-hui, WANG Ru ( College of Energy Source and Power Engineering, Jiangsu University, Zhenjiang, China, Post Code: 212013), GUI Ke-ting, SHI Ming-heng ( College of Energy Source and Environment, Southeast University, Nanjing, China, Post Code: 210096) // Journal of Engineering for Thermal Energy & Power. - 2016, 31(9). - 33 ~ 38

For the saturated flow and boiling heat exchange of a surfactant water solution in a microscale, a VOF ( volume of fluid) model and a user-defined function were used to conduct a numerical simulation of the saturated flow and boil-